

Molar Extinction Coefficient of Single-Wall Carbon Nanotubes

Friedrich Schöppler, Christoph Mann, Tilman C Hain, Felix Neubauer, Giulia Privitera, Francesco Bonaccorso, Daping Chu, Andrea C Ferrari, and Tobias Hertel

J. Phys. Chem. C, **Just Accepted Manuscript** • DOI: 10.1021/jp205289h • Publication Date (Web): 22 June 2011

Downloaded from <http://pubs.acs.org> on June 26, 2011

Just Accepted

“Just Accepted” manuscripts have been peer-reviewed and accepted for publication. They are posted online prior to technical editing, formatting for publication and author proofing. The American Chemical Society provides “Just Accepted” as a free service to the research community to expedite the dissemination of scientific material as soon as possible after acceptance. “Just Accepted” manuscripts appear in full in PDF format accompanied by an HTML abstract. “Just Accepted” manuscripts have been fully peer reviewed, but should not be considered the official version of record. They are accessible to all readers and citable by the Digital Object Identifier (DOI®). “Just Accepted” is an optional service offered to authors. Therefore, the “Just Accepted” Web site may not include all articles that will be published in the journal. After a manuscript is technically edited and formatted, it will be removed from the “Just Accepted” Web site and published as an ASAP article. Note that technical editing may introduce minor changes to the manuscript text and/or graphics which could affect content, and all legal disclaimers and ethical guidelines that apply to the journal pertain. ACS cannot be held responsible for errors or consequences arising from the use of information contained in these “Just Accepted” manuscripts.



Molar Extinction Coefficient of Single-Wall Carbon Nanotubes

Friedrich Schöppler,^a Christoph Mann,^a Tilman C. Hain,^a Felix M. Neubauer,^a Giulia Privitera,^b

*Francesco Bonaccorso,^b Daping Chu,^b Andrea C. Ferrari,^b and Tobias Hertel^{*a}*

^a Institute of Physical and Theoretical Chemistry, Department of Chemistry and Pharmacy, Julius-
Maximilians University of Würzburg, D-97074 Würzburg, Germany

^b Department of Engineering, University of Cambridge, Cambridge, CB3 0FA, U.K.

*tobias.hertel@uni-wuerzburg.de

**RECEIVED DATE (to be automatically inserted after your manuscript is accepted if required
according to the journal that you are submitting your paper to)**

1
2 **ABSTRACT** The molar extinction coefficient of single-wall carbon nanotubes (SWNTs) is determined
3
4 using fluorescence tagging, as well as AFM imaging, which facilitate correlation of nanotube
5
6 concentrations with absorption spectra. Tagging of SWNTs is achieved using fluorescence labeled
7
8 single strand DNA oligomers as dispersion additive, while AFM imaging is used to determine the mass
9
10 of SWNTs in the retentate of vacuum filtered colloidal SWNT suspensions. The resulting absorption
11
12
13
14
15
16 cross section for the first exciton transition of (6,5) nanotubes of $1.7 \cdot 10^{-17} \text{ cm}^2$ per C-atom corresponds
17
18
19
20
21
22
23
24
25 to an extinction coefficient of $(4400 \pm 1000) \text{ M}^{-1} \cdot \text{cm}^{-1}$ which is equivalent to an oscillator strength of
26
27 0.010 per carbon atom.
28
29
30
31
32
33
34
35
36
37
38
39
40
41
42
43
44
45
46
47
48
49
50
51
52
53
54
55
56
57
58
59
60

INTRODUCTION

1
2
3 The concentration of nanoparticles in suspensions is crucial for many kinetic phenomena with
4
5 chemical or photophysical nature but the measurement of particle concentrations is often fraught with
6
7 large and undesirable uncertainties. In contrast, absorption cross sections and the corresponding molar
8
9 extinction coefficients of molecular systems are generally better known and allow a reliable
10
11 determination of molecular concentrations in solutions. Moreover, the oscillator strength of optical
12
13 transitions – closely related to the extinction coefficient and frequently just as poorly characterized for
14
15 nanoparticle systems – represents one of the most fundamental characteristics of optically active systems
16
17 and allows key insights into the character of excited states. As a consequence, extinction coefficients
18
19 and oscillator strengths of nanomaterials are often debated, due to inherent difficulties with the
20
21 determination of nanoparticle concentrations in suspensions.
22
23
24

25
26 Here, we use fluorescence labeling and atomic force microscopy (AFM) for the determination of
27
28 single-wall carbon nanotube (SWNT) concentrations in aqueous suspension. A comparison with
29
30 previously published data suggests that some studies may have overestimated SWNT concentrations by
31
32 up to a factor of 30.¹⁻⁶ A measurement of the absorption cross section with greater confidence is thus
33
34 clearly desirable in particular since it is also essential for the determination of other photophysical
35
36 properties such as exciton size⁷ or diffusion coefficients.⁸ Comparative studies of photoluminescence
37
38 action cross sections - a product of absorption cross section and photoluminescence (PL) quantum yield
39
40 (QY) – would also benefit from greater confidence regarding the magnitude of absorption cross
41
42 sections.⁹
43
44
45

46
47
48
49 The first reports of SWNT absorption cross sections by Islam et al., cited $0.08 \cdot 10^{-17} \text{ cm}^2$ per C-atom
50
51
52
53
54
55
56
57
58 for the second subband S_2 transitions.¹ However, the samples used in that study were most likely heavily
59
60

1 aggregated^{10,11} and spectrally congested, which makes a determination of oscillator strengths difficult.
2
3 Another study using DNA-suspended and (6,5) enriched SWNTs by Zheng et al. gives an absorption
4
5
6
7 cross section for first subband S_1 excitons of $0.7 \cdot 10^{-17} \text{ cm}^2$ per C-atom.² A recent Rayleigh scattering
8
9
10
11
12
13
14
15
16
17
18
19 investigation finds an S_2 cross section of $2.5 \cdot 10^{-17} \text{ cm}^2$ per C-atom.⁶ As a side note we recall that at
20
21
22
23
24
25
26
27
28 normal incidence graphene is known to absorb 2.3% per layer in the same spectral range as the S_1
29
30 exciton feature of (6,5) SWNTs studied here.^{12,13} This corresponds to a photoabsorption cross section of
31
32
33
34
35 $0.6 \cdot 10^{-17} \text{ cm}^2$ per C-atom.
36
37
38
39
40
41
42
43

44 In the following, we discuss the determination of SWNT exciton absorption cross sections using two
45
46 independent techniques for the assessment of nanotube concentrations: 1) fluorescence labeling and 2)
47
48 AFM imaging of vacuum filtered SWNT retentate. In addition, and in contrast to several previous
49
50 studies of absorption cross sections,¹⁻⁶ the SWNTs used for our investigations are isolated monomers,
51
52 highly (6,5) enriched, to avoid ambiguities with the interpretation of congested spectra.
53
54
55
56
57

58 EXPERIMENTAL SECTION 59 60

1 For fluorescence labeling experiments we use 6-Carboxyfluorescein (FAM) labeled single strand
2 DNA of the $(GT)_{n=16}$ type (FAM-DNA). One mg of SWNT soot from the CoMoCat process¹⁴ is
3 dispersed in 3 ml phosphate buffered saline (PBS) HPLC water by ultrasonication with 16 μ M FAM-
4 DNA oligomer solution. The resulting dark suspension is ultracentrifuged for 18 h at 288,000 g in a
5 density gradient¹⁵ in order to sort nanotubes by diameter, as well as to remove nanotube aggregates,
6 residual catalyst and other contaminants.¹⁰ SWNT fractions are filtered 20 times with centrifugal filters
7 (Amicon Ultra, Milipore) to remove any excess of free FAM-DNA. The absorption spectrum of the
8 resulting purple suspension is dominated by the S_1 and S_2 exciton transitions of the (6,5) SWNT at
9 991 nm and 575 nm,¹⁶ respectively (see supporting information(SI)). Assuming similar absorption cross
10 section for different chiralities, the relative abundance of the (6,5) species is estimated to be about 85%-
11 90% of all semiconducting nanotubes.
12
13
14
15
16
17
18
19
20
21
22
23
24
25
26
27

28 RESULTS AND DISCUSSION

29
30
31 Fluorescence spectra of a 5.0 nM suspension of free FAM-DNA oligomer and of a SWNT sample
32 with SWNT-bound FAM-DNA are shown in the inset of Figure 1. A comparison of integrated PL
33 intensities of the free FAM-DNA solution with FAM-DNA-SWNT conjugates allows us to determine
34 the FAM-DNA concentration in the SWNT suspension if differences in PL QY are taken into
35 consideration. In FigureFigure 1 we also reproduce time-correlated single photon counting traces from
36 both free and SWNT-bound FAM-DNA. These allow to account for changes of the PL QY when
37 calculating FAM-DNA-SWNT conjugate concentrations. The PL decay of adsorbed FAM-DNA is
38 found to be bi-exponential - in agreement with previous investigations¹⁷ - with an average lifetime of
39 0.68 ns, while the free fluorophore decays with an average lifetime of 1.72 ns. This corresponds to a
40 61% decrease of the PL-QY of the adsorbed- with respect to the free fluorophore. For the FAM-DNA-
41 SWNT conjugate sample in Figure 1 this yields the concentration of surface bound FAM-DNA of 24
42 nM.
43
44
45
46
47
48
49
50
51
52
53
54
55
56
57
58
59
60

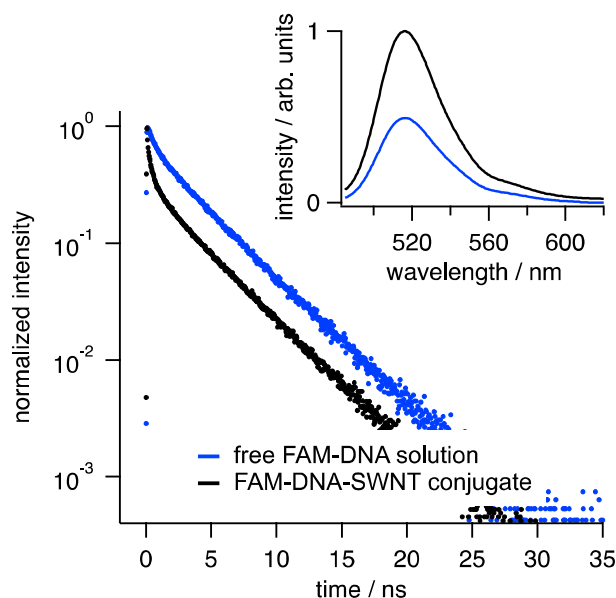


Figure 1. Time resolved fluorescence spectra of a fluorophore FAM-DNA solution and of FAM-DNA-SWNT conjugates. Emission from the adsorbed FAM-DNA is found to be less efficient than for the free fluorophore. The inset shows emission spectra of free and surface bound FAM-DNA for determination of the concentration of adsorbed DNA in the nanotube suspension.

For the conversion of the concentration of adsorbed FAM-DNA to a SWNT concentration we need to determine the DNA - SWNT stoichiometry, as given by the DNA number density ρ per tube unit length. The latter is related to θ , the fraction of the tube surface covered by DNA, the wrapping angle φ between DNA strand orientation and the tube axis, and the DNA oligomer length l by $\rho = \theta / (l \cdot \cos(\varphi))$ (see SI). Molecular dynamics calculations for a (11,0) SWNT indicate that the helical pitch of DNA wrapped around SWNTs is constrained by steric and Coulomb interactions and by the flexibility of the DNA backbone and lies between 8 nm and 10 nm, corresponding to wrapping angles of 25° and 30°, respectively.¹⁸ In combination with the range of anticipated phosphor-phosphor distances of 0.56-0.70 nm in the DNA backbone¹⁸⁻²⁰ this suggests that adsorbed (GT)_{n=16} will cover a region on the tube surface $l \cdot \cos(\varphi)$ between 16 nm and 20 nm in length. Due to steric constraints, it is unlikely that more than one DNA strand can bind to the same segment of a small diameter SWNT.¹⁸

The coverage θ needs to be assessed independently. Here, this is done experimentally using frequency shifts of the S_1 exciton caused by adsorption of an anionic surfactant (sodium cholate, SC) on bare

nanotube sections. These frequency shifts - on the order of a few nm - can be analyzed using a heterogeneous adsorption model (see Figure 2 and SI). First, the absorption wavelengths of density gradient ultracentrifugation (DGU) enriched, purely DNA covered and purely SC covered surfaces of $\lambda_{\text{DNA}} = 991 \text{ nm}$ and $\lambda_{\text{SC}} = 982 \text{ nm}$, respectively are measured independently. To first order the exciton peak position λ_{expt} after addition of SC to a DNA-SWNT conjugate suspension is then given by linear interpolation of the known absorption wavelengths of the pure phases in the ternary DNA-SC- H_2O system (see SI). Here this interpolation is done using the arithmetic mean of the exciton transitions in the pure phases and we have $\lambda_{\text{expt}} = \theta\lambda_{\text{DNA}} + (1-\theta)\lambda_{\text{SC}}$. If 2 wt% SC is added to a freshly prepared and ultracentrifuged DNA-SWNT conjugate suspension, we find a strong blue-shift upon SC addition from 991 nm to 984 nm indicating that only a fraction of the tubes ($\sim 20\%$) is covered with DNA after DGU. This is in good agreement with published estimates of $\sim 25\%$.²¹ If the freshly prepared DNA-SWNT suspension is saturated after fractionation by addition of excess DNA, the absorption wavelength is slightly shifted to 989 nm, indicating that the DNA coverage in this case is $\sim 80\%$.

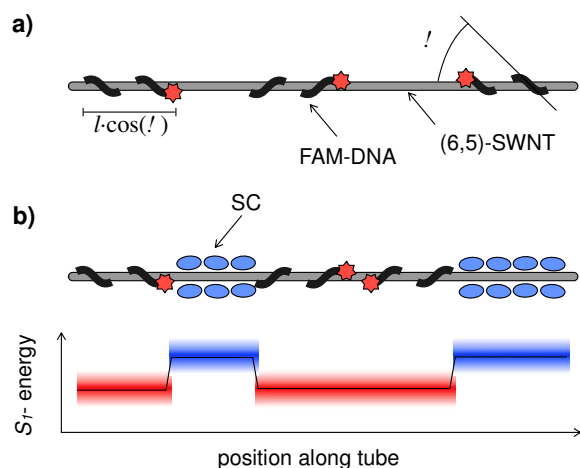


Figure 2. a) Schematic illustration of a partially DNA covered nanotube. b) Absorption of excitons in regions covered by DNA oligomers and those accessible to anionic surfactant, such as SC, are characterized by slightly different center wavelengths. This is used to assess the degree of SWNT saturation with DNA from optical absorption spectra.

1
2 The resulting absorption cross section for DNA suspended SWNTs then becomes $(2.3 \pm 0.7) \cdot 10^{-17} \text{ cm}^2$
3
4
5
6
7
8
9

10
11 per C-atom (see SI). The largest uncertainty of about 30% here arises from the determination of the
12
13 DNA surface coverage.
14

15
16 Next we use AFM imaging of the retentate from vacuum filtered SWNT suspensions to determine
17
18 SWNT concentrations. Here, SWNT suspensions are prepared by DGU with SC and sodium dodecyl
19
20 sulfate (SDS) surfactant mixtures.^{10,11,22} The resulting (6,5) enriched suspensions are diluted with
21
22 surfactant solution to an optical density (*OD*) in the S_1 transition range of about 10^{-4} . One ml of the
23
24 diluted suspension then undergoes vacuum filtration through cellulose filters with 0.1 micron pore size.
25
26 The briefly dried retentate is washed with DI water before being transferred to Si substrates for AFM
27
28 investigation (see SI).
29
30
31

32
33 AFM images from sparsely SWNT covered Si surfaces, such as in Figure 3, reveal that the filtration
34
35 process yields both, individual and aggregated SWNTs. The AFM images are used to measure length
36
37 and center height of single tubes, tube aggregates or aggregate sections. This allows us to determine the
38
39 total volume of SWNTs in the retentate. For the calculation of aggregate volume we assume close
40
41 packing, with a lattice constant of 1.1 nm, and nearly spherical aggregate cross sections. Considering a
42
43 variety of aggregate geometries then yields the following estimate of height to aggregate size
44
45 relationships: 0.62 nm - 1.58 nm: 1.5 tubes; 1.59 nm - 2.53 nm: 4.2 tubes; 2.54 nm - 3.48 nm: 7.2 tubes;
46
47 3.49 nm - 4.33 nm: 11.5 tubes (see Figure 3). The average tube number per aggregate is expected to be
48
49 slightly smaller since aggregates tend to taper off toward their ends, whereas our calculation assumes a
50
51 homogeneous aggregate diameter over the measured segments. The absorption cross section, σ , is then
52
53 determined from the *OD* of the filtered sample volume V_s and the length d of the optical path in the
54
55 spectrometer cell:
56
57
58
59
60

$$\sigma = \frac{ODV_s \ln(10)}{88 \text{nm}^{-1} N_T L_T d}$$

where the product of number and length of tubes, N_T and L_T with 88 corresponding to the number of atoms in the suspension (88 is the number of carbon atoms per nm length of a (6,5) SWNT). From the average over 38 AFM images with $25 \mu\text{m}^2$ area each, and with a total of 952 single tubes or tube aggregates, we obtain an absorption cross section of the S_1 exciton in SC suspension of $1.1 \cdot 10^{-17} \text{cm}^2$,

with an estimated uncertainty of 20%.

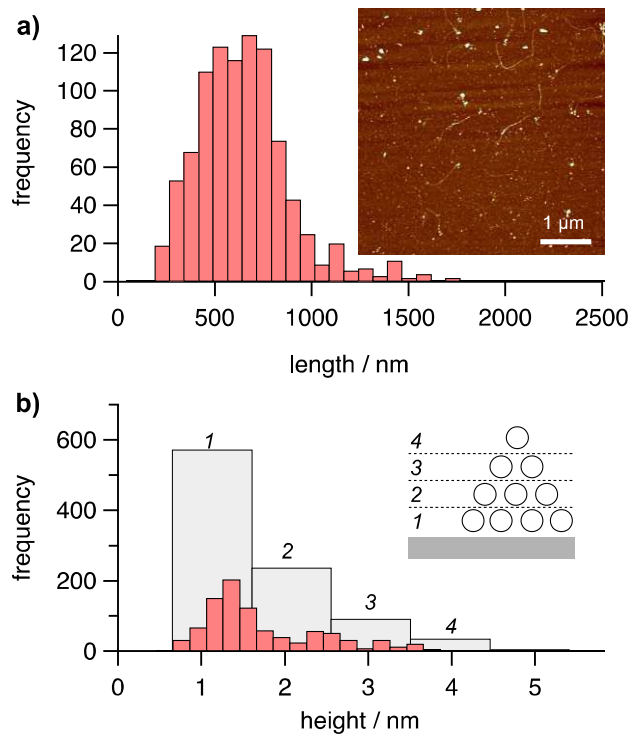


Figure 3. a) Aggregate length and b) height histograms obtained from the structures found in 38 AFM images of sparse retentates. The inset in a) shows an AFM image of a sparse SWNT retentate after transfer from a cellulose filter membrane to a Si substrate.

Unfortunately, the two absorption cross sections obtained from fluorescence labeling and AFM imaging experiments do not fall within their respective margins of error. This suggests that some systematic and perhaps some statistical uncertainties are not unaccounted for by the error analysis. Without a better understanding of the origin of these uncertainties however we cannot give preference to either of the two values and in the following discussion will thus use the average cross section of $1.7 \cdot 10^{-17} \text{ cm}^2$ per C-atom. Based on the variation of our results for different preparation runs and samples,

we estimate that the uncertainty associated with this value is $\sim 0.4 \cdot 10^{-17} \text{ cm}^2$ per C-atom. Other sources of uncertainty could be a possible overestimation of the DNA coverage on SWNT surfaces in the fluorescence labeling experiments, or a possible loss of SWNT material during sample transfer to the Si substrate for the AFM study. For both experiments this would imply that the measured cross section represents an upper bound. As discussed further below we will show that the value is in good agreement with expectations based on theoretical predictions of the exciton size.

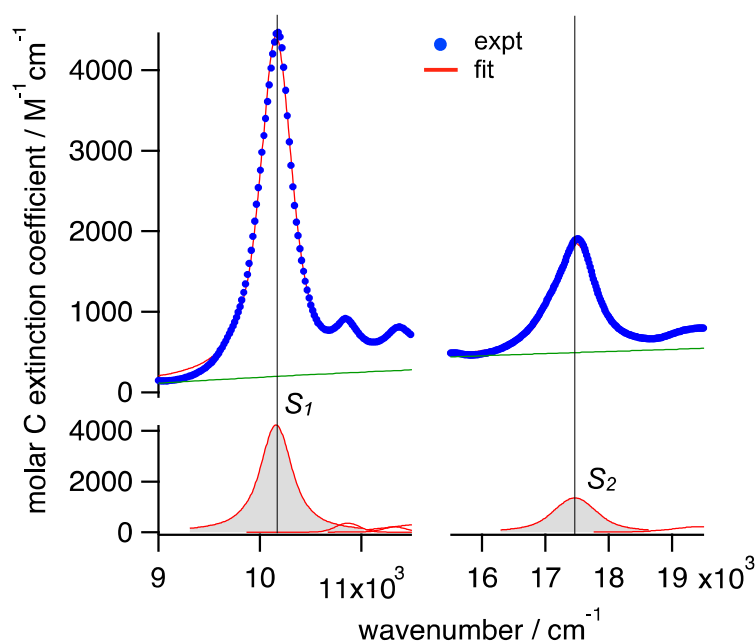


Figure 4. Calibrated absorption spectra of a (6,5) enriched SWNT suspension. The oscillator strengths of the S_1 and S_2 transitions are obtained from integration over the Voigt profiles in the lower part of the figure.

The absorption cross section is used to calculate the molar extinction coefficient of (6,5) SWNTs at the maximum of the S_1 exciton of $4400 \text{ M}^{-1}\cdot\text{cm}^{-1}$. Integration over the S_1 and S_2 exciton absorption

features shown in Figure 4 then yields transition strengths of $2.4\cdot 10^9 \text{ mol}^{-1}\cdot\text{cm}$ and $1.4\cdot 10^9 \text{ mol}^{-1}\cdot\text{cm}$,

respectively ($\text{M}^{-1}\cdot\text{cm}^{-1} = \text{L}\cdot\text{mol}^{-1}\cdot\text{cm}^{-1} = 1000 \text{ cm}^2\cdot\text{mol}^{-1}$). These integrals can be used to calculate the oscillator strength of the corresponding transitions from:^{23,24}

$$f = \frac{4\varepsilon_0 c^2 m_e \ln(10)}{N_A e_0^2} \int \varepsilon(\tilde{\nu}) d\tilde{\nu}$$

where ε_0 is the free space permittivity, c is the speed of light, m_e the electron mass, N_A is Avogadro's number, e_0 the elementary charge, $\varepsilon(\square)$ the molar extinction coefficient and \square the wavenumber (in cm^{-1}).

¹).²³ The constants leading the integral become $4.319\cdot 10^{-12} \text{ mol}\cdot\text{cm}^{-1}$. The resulting oscillator strengths

per C atom are 0.010 and 0.006 for the S_1 and S_2 exciton transitions, respectively. In combination with the transition linewidth, Δ_{FWHM} , this can also be used to establish a convenient relationship between c_C , the carbon atom concentration in suspension (in mol/L), and the OD of the S_1 transition according to:

$$c_C = B \frac{\Delta_{\text{FWHM}} OD}{f d}$$

1 where d is the thickness of the optical cell and f the C atom oscillator strength. For convenience the
2
3
4
5 constant $B = 5.1 \cdot 10^{-4} \text{ mol} \cdot \text{L}^{-1} \cdot \text{cm} \cdot \text{nm}^{-1}$ is calculated for the use with units typically utilized in the lab,
6
7
8
9
10
11
12
13
14 *i.e.*, the FWHM is given in nm and the spectrometer cell thickness in cm. Care needs to be taken to
15
16 ensure that the measurement of the FWHM is not affected by spectral congestion. In addition one needs
17
18 to bear in mind that oscillator strengths may depend to a varying degree on solvent, surfactant, possible
19
20 tube filling and the state of aggregation.
21
22

23 The exciton oscillator strengths and absorption cross sections determined above are larger than most
24
25
26
27
28 previous estimates with values ranging from $2.9 \cdot 10^{-18} \text{ cm}^2$ to $0.7 \cdot 10^{-17} \text{ cm}^2$ per C-atom for the $S_1^{2,5}$ and
29
30
31
32
33
34
35
36
37
38
39 from $2.4 \cdot 10^{-19} \text{ cm}^2$ to $0.5 \cdot 10^{-17} \text{ cm}^2$ per C-atom for the S_2 transition.^{1,3,4} All values are here adjusted for
40
41
42
43
44
45
46
47
48
49 irradiation with unpolarized light which is equivalent to irradiation of randomly oriented nanotubes with
50
51 linearly polarized light. If the exciting light is polarized in the direction of the transition dipole parallel
52
53 to the nanotube axis, these absorption cross sections have to be multiplied by a factor of 2. The results
54
55 presented here provide a new determination of absorption cross sections that benefits from the use of
56
57 highly enriched nanotube samples with little or no spectral congestion as well as from the use of two
58
59
60

independent approaches for the determination of SWNT concentrations, with similar results obtained for both types of experiments.

In addition to providing a useful means for the determination of nanotube concentrations in aqueous suspensions from absorption spectra, these results also allow an assessment of exciton size using the relationship between absorption oscillator strength and radiative lifetimes. Without knowledge of the concentration of a solution, its *OD* generally allows the determination of the total absorption cross-section and, in combination with the transition linewidth, of the total oscillator strength of a system. If the fluorophore concentration is known one can use this for a calculation of the fluorophore oscillator strength as well as the corresponding radiative lifetime τ_{rad} using:^{23,24}

$$\frac{1}{\tau_{\text{rad}}} = A_{\text{ab}} = \frac{2\pi e_0^2 n^2 g_a f}{\epsilon_0 m_e c \lambda^2 g_b}$$

Here $n = 1.33$ is the refractive index of water at 982 nm and g_a and g_b are the ground and excited state degeneracies. We use the radiative exciton lifetime of (1.6 ± 0.3) ns²⁵ to reverse this argument and estimate the fluorophore concentration from the total oscillator strength. From the above radiative exciton lifetime we obtain an S_1 oscillator strength of 5. The oscillator strength of 0.010 on a per-atom basis thus suggests that 500 C-atoms contribute to the coherent exciton oscillation. For the (6,5) tube with 88 C atoms per nm length, and using a Gaussian exciton envelope function,²⁶ with $\psi(z_e, z_h) \propto \exp(-(z_e - z_h)^2 / 2s^2)$ this yields an electron-hole correlation length s of $(500/88)/\sqrt{\pi}$ nm = 3.2 nm, in good agreement with previously measured and calculated exciton sizes ranging from 2.0 nm to ~3 nm.^{7,26,27} In fact this underlines that the above S_1 oscillator strength is consistent with the current theoretical understanding of the nature and properties of SWNT excitons.

CONCLUSION:

We estimated the molar extinction coefficients and oscillator strengths of the S_1 exciton in (6,5) SWNTs using two different approaches for determining carbon nanotube concentrations in colloidal suspensions. One approach is based on fluorescence labeling, while the other one makes use of AFM

1 imaging of vacuum filtered SWNTs on a Si wafer. The results allow to determine the molar C extinction
2
3
4
5 coefficient of the S_1 exciton in (6,5) SWNTs of $(4400 \pm 1000) \cdot \text{M}^{-1} \cdot \text{cm}^{-1}$, which corresponds to a C
6
7
8
9
10
11
12
13
14
15
16 absorption cross section of $(1.7 \pm 0.4) \cdot 10^{-17} \text{ cm}^2$ or an oscillator strength of 0.010. This oscillator strength
17
18
19
20
21
22
23
24
25
26 can be used in combination with the previously measured radiative S_1 lifetime of 1.6 ns for a new
27
28 determination of the S_1 exciton size of (6,5) SWNTs of 3.2 nm, which is confirmed by previous
29
30 experimental and theoretical studies.
31

32
33 **ACKNOWLEDGMENT** FB acknowledges funding from a Newton International Fellowship. ACF
34
35 from the ERC grant NANOPOTS, and a Royal Society Brian Mercer Award for Innovation and a Royal
36
37 Society Wolfson Research Merit Award.
38
39
40

41 **Supporting Information Available:** Absorption spectra of DGU enriched DNA-FAM- SWNT
42
43 samples; Geometrical considerations for determination of the length of a SWNT segment covered by a
44
45 single strand DNA oligomer; DNA coverage; Optical absorption and absorption cross section; Vacuum
46
47 filtration; Atomic force microscopy characterization; This material is available free of charge via the
48
49 Internet at <http://pubs.acs.org>.
50
51

52 53 54 **REFERENCES**

55
56
57 (1) Islam, M. F.; Milkie, D. E. C.; Kane, L.; Yodh, A. G.; Kikkawa, J. M. *Phys.Rev.Lett.*, **2004**, *93*(3)
58
59 037404.
60

- 1
2
3
4
5
6
7
8
9
10
11
12
13
14
15
16
17
18
19
20
21
22
23
24
25
26
27
28
29
30
31
32
33
34
35
36
37
38
39
40
41
42
43
44
45
46
47
48
49
50
51
52
53
54
55
56
57
58
59
60
- (2) Zheng, M.; Diner, A. *J. Am. Chem. Soc.*, **2004**, *126*, 15490.
- (3) Schneck, J. R.; Walsh, A. G.; Green, A. A.; Hersam, M. C.; Ziegler, L. D.; Swan, A. K. *J. Phys. Chem. A*, TBP
- (4) Berciaud, S.; Cognet, L.; Lounis, B. *Phys. Rev. Lett.*, **2008**, *101*(7), 077402-1.
- (5) Carlson, L. J.; Maccagnano, S. E.; Zheng, M.; Silcox, J.; Krauss, T. D. *Nano Lett.*, **2007**, *7*(12), 3698.
- (6) Joh, D. Y.; Kinder, J.; Herman, L. H.; Ju, S. Y.; Segal, M. A.; Johnson, J. N.; Chan, G. K. L.; Park, J. *Nat. Nanotech.*, **2011**, *6*, 51.
- (7) Luer, L.; Hoseinkhani, S.; Polli, D.; Crochet, J.; Hertel, T.; Lanzani, G. *Nat. Phys.*, **2009**, *5*, 54.
- (8) Wang, F.; Dukovic, G.; Brus, L. E.; Heinz, T. F. *Science*, **2005**, *308*, 838.
- (9) Tsyboulski, D. A.; Rocha, J. R.; Bachilo, S. M.; Cognet, L.; Weisman, R. *Nano Lett.*, **2007**, *7*(10), 3080.
- (10) Crochet, J.; Clemens, M.; Hertel, T. *J. Am. Chem. Soc.*, **2007**, *129*(26), 8058.
- (11) Bonaccorso, F.; Hasan, T.; Tan, P. H.; Sciascia, C.; Privitera, G.; Di Marco, G.; Gucciardi, P. G.; Ferrari, A. C. *J. Phys. Chem. C*, **2010**, *114*, 17267.
- (12) Mak, K. F.; Sfeir, M. Y.; Wu, Y.; Lui, C. H.; Misewich, J. A.; Heinz, T. F. *Phys. Rev. Lett.*, **2008**, *101*, 196405.
- (13) Nair, R. R.; Blake, P.; Grigorenko, A. N.; Novoselov, K. S.; Booth, T. J.; Stauber, T.; Peres, N. M. R.; Geim, A. K. *Science* **2008**, *320*, 1308.
- (14) Kitiyanan, B.; Alvarez, W. E.; Harwell, J. H.; Resasco, D. E. *Chem. Phys. Lett.*, **2000**, *317*, 497.
- (15) Arnold, M. S.; Stupp, S. I.; Hersam, M. C. *Nano Lett.*, **2005**, *5*, 713.

- 1 (16) Weisman, R. B.; Bachilo, S. M. *Nano Lett.*, **2003**, *3*(9), 1235.
2
3
4 (17) Alvarez-Pez, J. M.; Ballesteros, L.; Talavera, E.; Yguerabide, J. *J. Phys. Chem. A*, **2001**, *105*,
5 6320.
6
7
8
9 (18) Johnson, R. R.; Johnson, A. T. C.; Klein, M. L. *Nano Letters*, **2008**, *8*(1), 69.
10
11
12 (19) Manohar, S.; Tang, T.; Jagota, A. *J. Phys. Chem. C*, **2007**, *111*, 17835.
13
14
15 (20) Manohar, S.; Mantz, A. R.; Bancraft, K. E.; Hui, C.; Jagota, A.; Vezenov, D. V. *Nano Lett.*, **2008**,
16 *8*(12), 4365.
17
18
19
20
21 (21) Jeng, E. S.; Moll, A. E.; Roy, A. C.; Gastala, J. B.; Strano, M. S. *Nano Lett.*, **2006**, *6*(3), 371.
22
23
24 (22) Arnold, M. S.; Green, A. A.; Hulvat, J. F.; Stupp, S. I.; Hersam, M. C. *Nat. Nano.* **2006**, *1*, 60.
25
26
27 (23) Strickler, S. J.; Berg, R. A. *J. Chem. Phys.*, **1962**, *37*(4), 814.
28
29
30 (24) Lewis, G. N.; Kasha, M. *J. Am. Chem. Soc.*, **1945**, *67*, 994.
31
32
33 (25) Hertel, T.; Himmelein, S.; Ackermann, T.; Stich, D.; Crochet, J. *ACS Nano*, **2010**, *4*, 7161.
34
35
36 (26) Capaz, R. B.; Spataru, C. D.; Beigi, S. I.; Louie, S. G. *Phys. Rev. B*, **2006**, *74*, 121401(R).
37
38
39 (27) Perebeinos, V.; Tersoff, J.; Avouris, P. *Phys. Rev. Lett.*, **2004**, *92*, 257402.
40
41
42
43
44
45

46 SYNOPSIS TOC

47
48
49
50
51
52
53
54
55
56
57
58
59
60

